

Synthesis of Bifunctional Au/Pt/Au Core/Shell Nanoraspberries for in Situ SERS Monitoring of Platinum-Catalyzed Reactions

Wei Xie,[†] Christoph Herrmann,[†] Karsten Kömpe,[‡] Markus Haase,[‡] and Sebastian Schlücker^{*,†}

[†]Department of Physics, [‡]Institute of Chemistry, University of Osnabrück, Barbarastr. 7, 49076 Osnabrück, Germany

S Supporting Information

ABSTRACT: The synthesis of bifunctional Au/Pt/Au nanoraspberries for use in quantitative in situ monitoring of platinum-catalyzed reactions by surface-enhanced Raman scattering (SERS) is presented. Highly convoluted SERS spectra of reaction mixtures can be decomposed into the contributions of distinct molecular species by multivariate data analysis.

Bifunctional nanoparticles integrate two formerly distinct functionalities into a single entity with superior and sometimes unprecedented properties. Au–Fe₃O₄ nanoparticles (NPs) represent an example for a hybrid system which exhibits both plasmonic (Au) and magnetic (Fe₃O₄) activity.¹ The combination of Au with metals such as Pd or Pt offers the attractive option for label-free in situ monitoring of Pd- or Pt-catalyzed reactions by using surface-enhanced Raman scattering (SERS).² Previous approaches to catalytically active NPs include either core/shell NPs in which only one metal component is exposed to the environment,³ or alloy NPs with decreased SERS activity.⁴ Pd/Au nanoshells comprising a silica core covered with a thin Au shell and Pd islands deposited on the Au shell represent one of the very few examples in which both functionalities, catalytic activity (Pd) and SERS activity (Au), are integrated into a single bifunctional entity.^{2b} Using a film of Pd/Au nanoshells on a Si wafer, the Pd-catalyzed hydro-dechlorination of a chlorinated solvent in water was monitored in situ by SERS.

Despite of the progress achieved during the last years, the following limitations for the application of SERS to in situ monitoring of catalytic reactions exist: (1) synthesis of complex hybrid metal nanostructures for in situ SERS, which possess both a high SERS activity and a large surface area of the catalytically active metal at the same time; (2) establishing in situ SERS for Pt-catalyzed reactions due to the central role and widespread use of platinum in catalysis; (3) monitoring reactions directly in colloidal suspension, in addition to existing approaches using NP films immobilized on a solid support; (4) quantification of components involved in the catalytic reaction via in situ SERS (this is important for evaluating the quality of novel catalysts, testing reaction mechanisms and establishing kinetic models); (5) identification of unknown species by in situ SERS; (6) bifunctional NPs for in situ SERS that are stable and active both catalytically and plasmonically even under harsh reaction conditions such as elevated temperatures.

Here, we present an integrated approach which overcomes all of these six limitations. Specifically, we demonstrate the in situ SERS monitoring of a platinum-catalyzed reaction via rationally

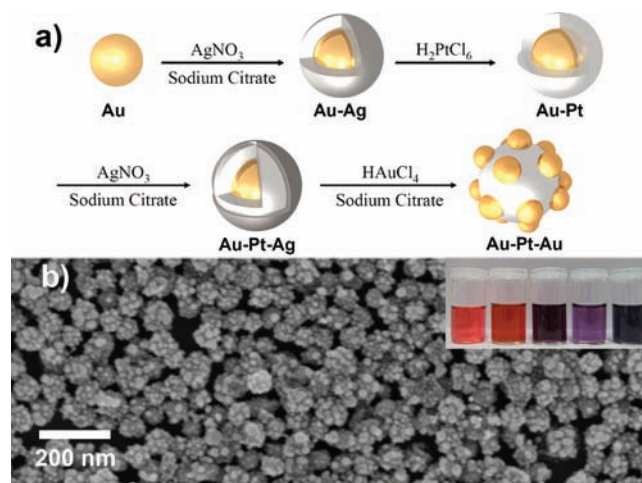


Figure 1. (a) Reaction scheme showing morphological and structural changes involved in the fabrication of Au/Pt/Au core/shell nanoraspberries and (b) SEM image of the product (Au/Pt/Au) (inset: photo of the colloids during different synthesis steps).

designed bifunctional, raspberry-like Au/Pt/Au core/shell particles with a high Pt surface area and a high plasmonic activity (criteria 1 and 2 from above). Experimental details of the synthesis, carried out in aqueous solution, can be found in the Supporting Information (SI). Their application to quantitative reaction monitoring of NO₂ reduction to NH₂ moieties via an azo intermediate by sodium borohydride (NaBH₄) in colloidal suspension by SERS is demonstrated, using non-negative matrix factorization (NMF) for multivariate spectral analysis (criteria 3 and 4). Since this combined quantitative spectroscopic/multivariate approach does not require any a priori information despite of the number of involved chemical components, it has the potential to also identify unknown chemical species occurring during catalysis (criterion 5). Finally, we also demonstrate that the raspberry-like Au/Pt/Au core/shell particles are stable even at elevated temperatures and, more importantly, that both their catalytic and SERS activity is still maintained (criterion 6).

Figure 1 depicts the synthesis route to raspberry-like Au/Pt/Au core/shell NPs (Figure 1a), together with their characterization by SEM (Figure 1b). The first step is the formation of a Ag shell around the Au core. The conversion from Au/Ag to Au/Pt core/shell particles is achieved via the galvanic replacement of Ag by Pt through the addition of hexa-chloroplatinic(IV) acid

Received: September 2, 2011

Published: November 04, 2011

(Figure S1, SI). Silver is deposited on the Pt surface in a second coating step, again using silver nitrate and sodium citrate as reducing agent. In the last step of the synthesis, raspberry-like Au/Pt/Au NPs are formed via the concerted action of both reagent reduction and galvanic replacement (*vide infra*). This approach leads to the growth of the desired Au protuberances instead of the formation of a complete and smooth Au shell.

The SEM picture in Figure 1b demonstrates that uniform and monodisperse Au/Pt/Au nanoraspberries with an average diameter of 86.7 ± 6.4 nm are obtained (Figure S2, SI). It is important to note that the complete and smooth Pt shell around the Au core (cf. TEM picture in Figure 2a) is a prerequisite for the subsequent steps leading to raspberry-like Au/Pt/Au NPs. First, a smooth Pt shell is required since it serves as a template for the Ag coating. Second, the Ag species is necessary for the subsequent growth of the Au protuberances in the Au/Pt/Au NPs.⁵ During the heterogeneous growth of the Au protuberances, Ag structures on the Pt surface (Figure S3, SI) are first dismantled by galvanic replacement of Ag by Au; this way, many growth points for Au are formed at the positions where Ag was located before. The subsequent epitaxial growth of the Au protuberances is assigned to (a) the Kirkendall effect associated with galvanic replacement, and (b) the deposition of Au atoms produced by reagent reduction onto the existing Au structures. Overall, this heterogeneous growth is a result of the combined action of both galvanic replacement and reagent reduction. In contrast, earlier methods for the synthesis of Pt nanostructures in aqueous media yielded highly branched morphologies,⁶ which are not suited here for obtaining the desired complex and bifunctional nanoarchitecture (criteria 1 and 2).

The formation of the hybrid nanoparticles is accompanied by changes in their morphological properties. Figure 2 shows TEM images of Au/Pt core/shell NP precursors (Figure 2a) and the final Au/Pt/Au raspberry-like NPs (Figure 2b), indicating both their monodispersity and the high reproducibility of the reaction. The growth of Pt via galvanic replacement presented here is much faster than the reagent reduction process, and the new structures inherit the shape of their templates. Generally, Pt/Au nanoparticles fabricated via reagent reduction exhibit highly branched Pt structures around the spherical Au core.⁷ In our case, we obtained a smooth Pt shell (Figure 2a) via galvanic replacement of the Ag shell of the spherical Au/Ag core/shell NPs (Figure 1a). The HR-TEM image of a single Au/Pt/Au raspberry-like NP (Figure 2c) clearly delineates the inner Au core from the surrounding Pt shell as well as the Au protuberances on top of it (cf. also the computer-generated 3D model in Figure 2d). The surface area of the nanoraspberry estimated via the model is ca. 2.3×10^{-14} m², comprising a Pt surface of ca. 8.3×10^{-15} m² (Figure S4, SI). At higher magnification, the crystallographic planes of cubic face-centered Au ($d = 2.36$ Å) and Pt ($d = 2.26$ Å) can be observed (Figure S5, SI). The elemental composition was determined by EDX spectroscopy (Figure S6, SI).

The presented Au/Pt/Au raspberry-like morphology is important for the bifunctional property comprising both SERS and Pt-catalytic activity: (1) the small plasmonic Au protuberances are required for SERS and, most importantly, the large catalytically active Pt surface area (Figure 2d) is accessible at the same time; (2) the Pt shell with a smooth surface is necessary for the growth of the small Au protuberances; (3) the large Au core acts as a template for the growth of the Pt shell and, more importantly, provides the required high SERS activity of the entire Au/Pt/Au

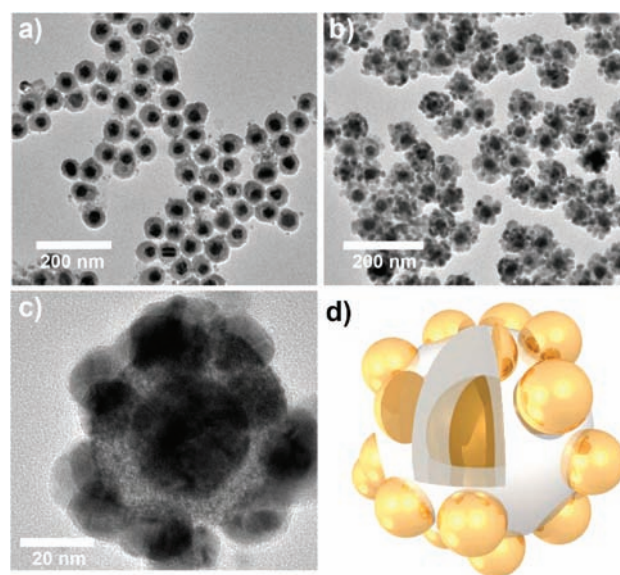


Figure 2. TEM images of (a) Au/Pt core/shell NPs, (b) Au/Pt/Au core/shell nanoraspberries and (c) a single nanoraspberry; (d) 3D model of the nanoraspberry shown in panel c.

NPs via plasmonic coupling with the small Au protuberances (Figure 2d). In contrast, without Au protuberances, no SERS activity is observed (*vide infra*).

The experimental demonstration that the Au/Pt/Au core/shell nanoraspberries from Figure 2 exhibit both catalytic and SERS activity requires the choice of a proper model reaction for this proof-of-concept study. Here, we examine the reduction of a nitro-aromatic compound to the corresponding aniline derivative (R–NH₂) by NaBH₄. Specifically, the educt of the reaction is a self-assembled monolayer (SAM) of 4-nitrothiophenol (4-NTP) on the surface of the Au/Pt/Au particles (present on both Au and Pt regions, cf. Figure 2d).⁸ Figure 3 (bottom) shows the SERS spectrum of 4-NTP as a SAM on the surface of the Au/Pt/Au core/shell nanoraspberries. The Raman band at ca. 1340 cm⁻¹ is assigned to the symmetric nitro stretching vibration, while the peaks at ca. 1080 and 1573 cm⁻¹ are due to phenyl ring modes. Positive SERS control experiments with a SAM of 4-NTP on solid Au nanospheres instead of Au/Pt/Au NPs yielded the same SERS spectrum (Figure S7, SI), demonstrating that Au has no or at least a very low catalytic activity in this case, in contrast to different but related reaction systems.⁹ Negative control experiments with Au/Pt core/shell NPs yielded no SERS signals, indicating that Pt is not SERS-active and that the small Au protuberances are required for SERS monitoring (*vide supra*). These results qualitatively confirm the high SERS activity of the Au/Pt/Au core/shell nanoraspberries. However, it is difficult to make reliable and stringent quantitative statements on the SERS enhancement factor for this complex nanostructure.¹⁰

For starting the catalytic reaction, different volumes of 10 mM aqueous NaBH₄ solution were added to the Au/Pt/Au particles covered with a SAM of 4-NTP and the corresponding SERS spectra were recorded directly after the addition. New vibrational Raman bands of an intermediate are observed upon NaBH₄ addition, which can be assigned to 4,4'-dimercapto-azobenzene (4,4'-DMAB).¹¹ The three peaks at 1143 , 1388 , and 1430 cm⁻¹ are due to C–N symmetric stretching, N=N stretching, and C–H in-plane bending modes, respectively.¹² With increasing NaBH₄ volume (from bottom to top in Figure 3), the

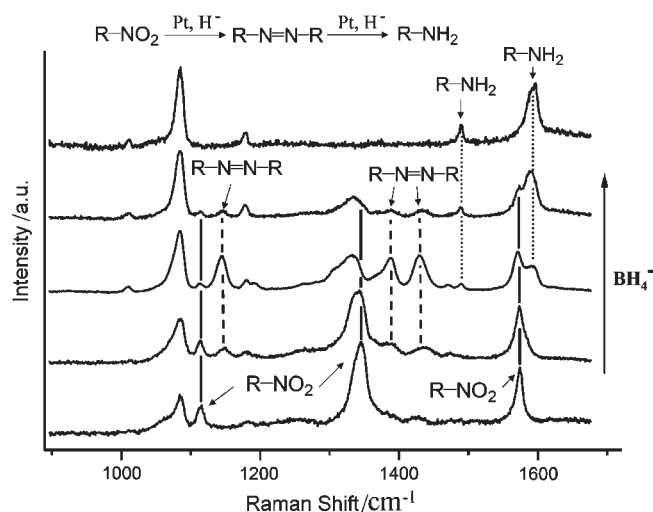


Figure 3. Raw SERS spectra recorded during the Pt-catalyzed hydride reduction of an aromatic nitro compound, using different amounts of the reducing reagent NaBH_4 . From bottom to top: increasing volumes of 10 mM NaBH_4 solution were added to 4-NTP-functionalized Au/Pt/Au core/shell nanoraspberries.

concentration of 4,4'-DMAB initially increases and then finally decreases. For large volumes of NaBH_4 , only additional bands of a third species are observed (Figure 3 top). These bands can be assigned to the corresponding aniline derivate R-NH_2 , in this case 4-aminothiophenol (4-ATP). 4-ATP is the final reaction product for the reduction of 4-NTP by NaBH_4 . Overall, a series of 10 SERS spectra was recorded (Figure S8, SI). Could it be possible that a mixture of bare Au and bare Pt nanospheres has the same capability of catalytic conversion as the Au/Pt/Au nanoraspberries? The answer is no: we found that in the case of the mixture, the catalytic reaction is not completed, even upon addition of the highest NaBH_4 volume (Figure S9, SI).

Quantitative in situ reaction monitoring by SERS requires the decomposition of the experimentally detected spectra into the individual contributions of the involved molecular species, in this case the educt (R-NO_2), intermediate (R-N=N-R), and final product (R-NH_2). The simplest approach is based on single parameters such as peak heights or areas. These univariate approaches can easily be implemented when the corresponding marker bands of the distinct species are spectrally well separated from each other. However, there is a severe spectral overlap between the contributions of all three species (Figure 4b). In contrast, multivariate evaluation schemes are based on the entire vibrational spectrum, rather than just a single parameter as in their univariate counterparts. We decided to use NMF since it has already been successively applied to the decomposition of highly convoluted UV resonance Raman spectra.¹³

The decomposition of the matrix with experimental data by NMF (Figure S10, SI) yields both the SERS spectra of the three pure components (Figure 4a) and their relative contributions (Figure 4b). Figure 4a also contains the assignment of the SERS spectra to the corresponding molecular species: 1 = 4-NTP, 2 = 4,4'-DMAB, and 3 = 4-ATP. They agree well with directly measured reference SERS data.¹¹ The relative concentrations plotted in Figure 4b contain normalized values, yielding a sum of 100% ($R = 1.0$). The mean and the standard deviation were calculated from three independent SERS measurements. The agreement between experimental spectra (mixtures) and

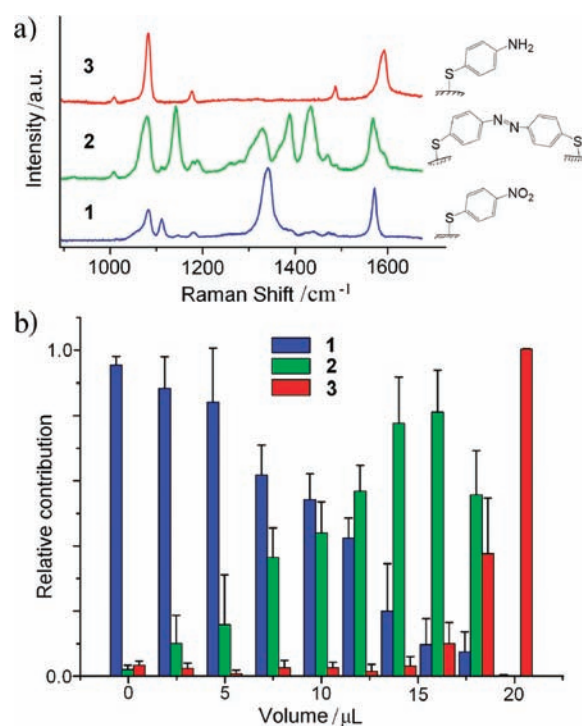


Figure 4. (a) NMF-calculated SERS spectra of the three pure components, together with their assignment to the three molecular species 4-NTP, 4,4'-DMAB, and 4-ATP. (b) Calculated relative contributions of the three pure components as a function of NaBH_4 volume.

calculated data (decomposition by NMF) is excellent and only very small residuals are observed (Figure S11, SI).

Overall, the concentration profile in Figure 4b suggests a sequential hydride reduction of 4-NTP to 4,4'-DMAB and finally to 4-ATP. More importantly, it provides quantitative information about their relative concentrations. It is also important to note again that no a priori information about the identity or even the molecular spectra of the individual species is required for this multivariate approach. The only input is the number of pure components (here: three) since this determines the matrix dimensions. In principle, also the SERS spectrum of any unknown species could be detected (criterion 5) in an explorative mode (Figure S12, SI).

Finally, we also tested both SERS and catalytic activity of the Au/Pt/Au nanoraspberries at an elevated reaction temperature (criterion 6). SERS spectra of 4-NTP-functionalized nanoraspberries before and after reduction recorded at 90 °C (Figure S13, SI) indicate that the bifunctional NPs are stable and exhibit the same SERS and catalytic activity even at this elevated temperature. This is particularly important for applying in situ quantitative SERS monitoring of catalytic reactions under harsh and realistic conditions.

In conclusion, we have demonstrated a straightforward method to fabricate Au/Pt bimetallic nanoparticles with two metal surfaces (Au and Pt) exposed, thereby integrating both SERS and catalytic activity into a single bifunctional unit. The Au/Pt/Au core/shell nanoraspberries synthesized here can also be used for in situ quantitative SERS monitoring of Pt-catalyzed reactions under realistic conditions. The presented multivariate approach for the quantitative decomposition of in situ SERS spectra allows to determine the chemical identity of the involved molecular species and to quantify their relative contributions, which is a

requirement for establishing reaction mechanisms (pure component spectra) and testing kinetic models (concentrations of pure components). Finally, we note that the presented approach of using bifunctional Au/Pt/Au nanoraspberries for SERS monitoring of Pt-catalyzed reactions is currently limited to molecular species containing a surface-seeking group in order to experience the necessary SERS enhancement.

■ ASSOCIATED CONTENT

S Supporting Information. Experimental details, NMF data processing method, TEM/HR-TEM images, EDX data, and SERS spectra. This material is available free of charge via the Internet at <http://pubs.acs.org>.

■ AUTHOR INFORMATION

Corresponding Author

sebastian.schluecker@uos.de

■ ACKNOWLEDGMENT

This work was supported by the Alexander von Humboldt Foundation in Germany. We thank Bernd Walkenfort for technical support.

■ REFERENCES

- (1) (a) Heng, Y.; Chen, M.; Rice, P. M.; Wang, S. X.; White, R. L.; Sun, S. H. *Nano Lett.* **2005**, *5*, 379. (b) Xu, C. J.; Xie, J.; Ho, D.; Wang, C.; Kohler, N.; Walsh, E. G.; Morgan, J. R.; Chin, Y. E.; Sun, S. H. *Angew. Chem., Int. Ed.* **2008**, *47*, 173. (c) Bao, F.; Yao, J. L.; Gu, R. A. *Langmuir* **2009**, *25*, 10782.
- (2) (a) Zou, S. Z.; Williams, C. T.; Chen, E. K. Y.; Weaver, M. J. *J. Am. Chem. Soc.* **1998**, *120*, 3811. (b) Heck, K. N.; Janesko, B. G.; Scuseria, G. E.; Halas, N. J.; Wong, M. S. *J. Am. Chem. Soc.* **2008**, *130*, 16592. (c) Kim, H.; Kosuda, K. M.; Van Duyne, R. P.; Stair, P. C. *Chem. Soc. Rev.* **2010**, *39*, 4820. (d) Guerrini, L.; Lopez-Tobar, E.; Garcia-Ramos, J. V.; Domingo, C.; Sanchez-Cortes, S. *Chem. Commun.* **2011**, 3174.
- (3) (a) Mazumder, V.; Chi, M. F.; More, K. L.; Sun, S. H. *Angew. Chem., Int. Ed.* **2010**, *49*, 9368. (b) Wang, L.; Yamauchi, Y. *J. Am. Chem. Soc.* **2010**, *132*, 13636.
- (4) Chen, J. Y.; Wiley, B.; McLellan, J.; Xiong, Y. J.; Li, Z. Y.; Xia, Y. N. *Nano Lett.* **2005**, *5*, 2058.
- (5) Xie, W.; Su, L.; Donfack, P.; Shen, A. G.; Zhou, X. D.; Sackmann, M.; Materny, A.; Hu, J. M. *Chem. Commun.* **2009**, 5263.
- (6) Lim, B.; Xia, Y. N. *Angew. Chem., Int. Ed.* **2011**, *50*, 76.
- (7) (a) Guo, S. J.; Wang, L.; Dong, S. J.; Wang, E. K. *J. Phys. Chem. C* **2008**, *112*, 13510. (b) Guo, S. J.; Li, J.; Dong, S. J.; Wang, E. K. *J. Phys. Chem. C* **2010**, *114*, 15337.
- (8) (a) Rosario-Castro, B. I.; Fachini, E. R.; Hernandez, J.; Perez-Davis, M. E.; Cabrera, C. R. *Langmuir* **2006**, *22*, 6102. (b) Silien, C.; Dreesen, L.; Cecchet, F.; Thiry, P. A.; Peremans, A. *J. Phys. Chem. C* **2007**, *111*, 6357.
- (9) (a) Kundu, S.; Lau, S.; Liang, H. *J. Phys. Chem. C* **2009**, *113*, 5150. (b) Zhou, X. C.; Xu, W. L.; Liu, G. K.; Panda, D.; Chen, P. *J. Am. Chem. Soc.* **2009**, *132*, 138.
- (10) Unknown parameters: (a) molar extinction coefficient; (b) exact surface area of the Au protuberances for each nanoraspberry; (c) degree of particle aggregation, leading to SERS signal enhancement.
- (11) Huang, Y. F.; Zhu, H. P.; Liu, G. K.; Wu, D. Y.; Ren, B.; Tian, Z. Q. *J. Am. Chem. Soc.* **2010**, *132*, 9244.
- (12) Wu, D. Y.; Zhao, L. B.; Liu, X. M.; Huang, R.; Huang, Y. F.; Ren, B.; Tian, Z. Q. *Chem. Commun.* **2011**, 2520.
- (13) (a) Srivastava, S. K.; Niebling, S.; Küstner, B.; Wich, P. R.; Schmuck, C.; Schlücker, S. *Phys. Chem. Chem. Phys.* **2008**, *10*, 6770. (b) Niebling, S.; Srivastava, S. K.; Herrmann, C.; Wich, P. R.; Schmuck, C.; Schlücker, S. *Chem. Commun.* **2010**, 2133. (c) Niebling, S.; Kuchelmeister, H. Y.; Schmuck, C.; Schlücker, S. *Chem. Commun.* **2011**, 568.